ACS APPLIED MATERIALS & INTERFACES

Research Article

www.acsami.org

Surface Complex Formation between Aliphatic Nitrile Molecules and Transition Metal Atoms for Thermally Stable Lithium-Ion Batteries

Young-Soo Kim,[†] Hochun Lee,[‡] and Hyun-Kon Song*[,†]

[†]Department of Energy Engineering and School of Energy and Chemical Engineering, UNIST, Ulsan 689-798, Korea

[‡]Department of Energy Systems Engineering, Daegu Gyeongbuk Institute of Science and Technology (DGIST), Daegu 711-873, Korea

Supporting Information

ABSTRACT: Non-flammability of electrolyte and tolerance of cells against thermal abuse should be guaranteed for widespread applications of lithium-ion batteries (LIBs). As a strategy to improve thermal stability of LIBs, here, we report on nitrile-based molecular coverage on surface of cathode active materials to block or suppress thermally accelerated side reactions between electrode and electrolyte. Two different series of aliphatic nitriles were introduced as an additive into a carbonate-based electrolyte: di-nitriles ($CN\text{-}[CH_2]_n\text{-}CN$ with n = 2, 5, and 10) and mono-nitriles ($CH_3\text{-}[CH_2]_m\text{-}CN$ with m = 2, 5, and 10). On the basis of the strong interaction between the electronegativity of nitrile functional groups and the electropositivity of cobalt in $LiCoO_2$ cathode, aliphatic mono- and di-nitrile molecules improved the thermal stability of lithium ion cells by efficiently protecting the surface of $LiCoO_2$. Three factors, the surface coverage θ, the steric hindrance of aliphatic moiety within nitrile molecule, and the chain polarity, mainly affect thermal tolerance as well as cell performances at elevated temperature.

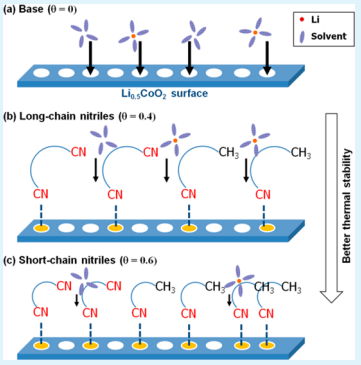

KEYWORDS: *thermal stability, aliphatic nitrile, electrolyte, cobalt surface, lithium-ion batteries*

INTRODUCTION

Lithium-ion batteries (LIBs), because of their high capacity of energy storage, have dominated energy storage markets for consumer electronics, electric vehicles, and even grid-connected renewable energy sources. The ever-increasing demand for higher energy density has aggressively pushed LIBs to the brink of electrochemical limitations. Cells have been designed to load more active materials within confined cell geometry[1−3] and higher energy density materials operating at high voltages have been developed.[4−7] However, these efforts have simultaneously triggered growing concerns in intrinsic safety because higher electric energy can thermodynamically be converted to the same amount of exothermic reactions if cells are subjugated to unexpected operational conditions or inadvertent abuse.

Volatility and flammability of conventional carbonate-based organic electrolytes make LIBs vulnerable to thermal shocks. They are easily decomposed or oxidized beyond 4 V when being contacted with charged active materials at elevated temperatures.[8] Resultantly, cells experience capacity fading with gas emission, dimensional distortion and problematic cycle life.[9,10] As one of the solutions to overcome the safety issues, the use of non-flammable[11] or flame-retardant electrolytes[12,13] has been considered. However, cell performances were not guaranteed as a result of the trade-off with thermal stability enhancement.

To prevent these defects induced by electrolytes, in our previous study, we demonstrated that the introduction of succinonitrile to electrolytes exhibited great improvements in both performance and safety at high temperature, modifying electrode-electrolyte interface by strong interaction between nitrile functional group (−CN) and Li_xCoO_2 ($0.5 < x < 1$) cathode surface.[14] The similar improvement of thermal stability was also observed in macromolecules containing cyanoethyl functional groups.[15] With these successful experiences with nitriles, we took into consideration that it would be a logically desirable choice of study to investigate the effects of molecular configuration of the compounds containing electron-rich nitrile groups on the surface chemistry between electrolytes and Li_xCoO_2 cathodes. However, few studies on thermal stability and correlation with performance in the nitrile-containing electrolytes have been found in literature except for some studies illustrating the effects of nitriles at high voltage[16,17] or high energy and power density.[18,19] In this work, we used mono-nitriles ($CH_3\text{-}[CH_2]_m\text{-}CN$ or $(1, m)$) and di-nitriles ($CN\text{-}[CH_2]_n\text{-}CN$ or $(2, n)$) with a variation of aliphatic chain length to study on the effects of the number of cyano groups (1 or 2) and the number of carbons (m or n) in the aliphatic chains. The surface coverage of the nitriles at the electrolyte−electrode interface is expected to depend on the molecular configuration.

EXPERIMENTAL SECTION

Electrolytes. Carbonate-based electrolytes with $LiPF_6$ lithium salt and fluoroethylene carbonate (FEC) as an additive were used as a base

Received: March 20, 2014
Accepted: May 17, 2014
Published: May 17, 2014

   dx.doi.org/10.1021/am501671p | ACS Appl. Mater. Interfaces 2014, 6, 8913−8920

electrolyte (Soul Brain; H_2O level ≤10ppm). Aliphatic mono-nitriles and di-nitriles (Acros) were added to the base electrolyte at 3 wt %. Molecules with three different lengths of aliphatic chains were used for each nitrile (Table 1). All chemicals were placed with molecular sieves before use. Electrolytes were prepared in a glove-box (MBraun, Germany; H_2O ≤1 ppm and O_2 ≤1 ppm).

Table 1. Composition of Carbonate-Based Electrolytes

notation	composition[a]
base	1 M $LiPF_6$ in EC:EMC (1:2 vol %) + 2 wt % FEC
(2 ,*n*)	base +3 wt % CN-$[CH_2]_n$-CN (*n* = 2, 5, 10)
(1, *m*)	base + 3 wt % CH_3-$[CH_2]_m$-CN (*m* = 2, 5, 10)

[a]EC, ethylene carbonate; EMC, ethylmethyl carbonate; FEC, fluoroethylene carbonate; *n* = 2, succinonitrile; *n* = 5, pimelonitrile; *n* = 10, dodecanedinitrile; *m* = 2, butyronitrile; *m* = 5, heptanenitrile; *m* = 10, dodecanenitrile.

Physicochemical Analysis. Ionic conductivity was measured in a temperature-controlled circulator by using a conductivity meter (Mettler-Toledo, SevenGo Duo pro). Viscosity of electrolytes was estimated by a viscometer (Brookfield, DV-II+ Pro with SC4-18 spindle), which was measured at least two times at a shear rate of 198 to 264 s^{-1} at a fixed temperature. The standard deviations of ionic conductivities and viscosities were estimated at less than 0.05 mS cm^{-1} and 0.06 cP, respectively, from at least more than three times repetitive measurements.

Electrochemical Analysis. Soft-packed $LiCoO_2$ (LCO)|graphite cells (760 mAh at its nominal capacity) were prepared with a separator of porous polyethylene (NH616, Asahi). Composition of cathodes was 95 wt % LCO (KD 10, Umicore), 2 wt % Super-P and 3 wt % polyvinylidene fluoride (PVDF) (KF1000, Kureha). Composition of anodes was 97.5 wt % natural graphite (P15BDH, Nippon Carbon), 1.5 wt % styrene−butadiene rubber (SBR) (BM400B, Zeon) and 1 wt % carboxy-methyl cellulose (CMC) (BSH12, Daichi). The electrodes were stacked and assembled into Al-laminated packages (Commercial-grade Al lamination sheet, DEL-40H, DNP). For stabilization, batteries were charged to 4.2 V (constant current/constant voltage with 5% cut-off of current) and discharged to 3 V (constant current) at a rate of 0.2*C* several times before evaluation.

Thermal Analysis. Thermally-induced reactions between electrolytes and cathodes were investigated in the range of 30 °C to 300 °C at 10 °C min^{-1} by differential scanning calorimetry (DSC; TA Instruments, Q100). Cathodes of charged full cells were used as specimen. The specimen were placed in high-pressure DSC cells (Perkin Elmer) sealed with gold−copper sheets in a dry room.

Electrochemical Impedance Measurement. The impedance spectra of cells fully charged at 4.2 V were obtained by applying 10 mV ac amplitude in the frequency range of 10 mHz to 200 kHz. All measurements were performed at 23 °C using a potentiostat (Biologic VSP) with built-in EIS analyser. Cells experiencing the thermal storage at 80 °C for 3 days were used. Before measurement, cells were charged and discharged at a rate of 0.2*C* to observe recovery efficiency.

X-ray Photoelectron Spectroscopy (XPS). Surface of cathodes were investigated by XPS. Charged full cells were disassembled and completely rinsed with EMC in a nitrogen-filled drybox. Then, the cathode samples placed on holders were transferred to a XPS spectrometer that is connected to the drybox through a transfer chamber without any exposure to air and/or moisture. K-alpha spectrometer (Thermo Fisher) was used with a focused monochromatized Al Kα radiation ($h\nu$ = 1486.6 eV). The analyzed area of each sample was 400 um^2. Peaks were recorded with constant pass energy of 50 eV. The binding energy was calibrated from the C 1s peak at 285 eV. The peak location and areas were optimized by a weighted least-square fitting method using Gaussian-Lorentzian summation.

RESULTS AND DISCUSSION

Basic Properties of Electrolytes. Ionic conductivity (σ) and viscosity (η) were investigated as a function of temperature in the presence and absence of aliphatic nitriles (Figure 1). As η

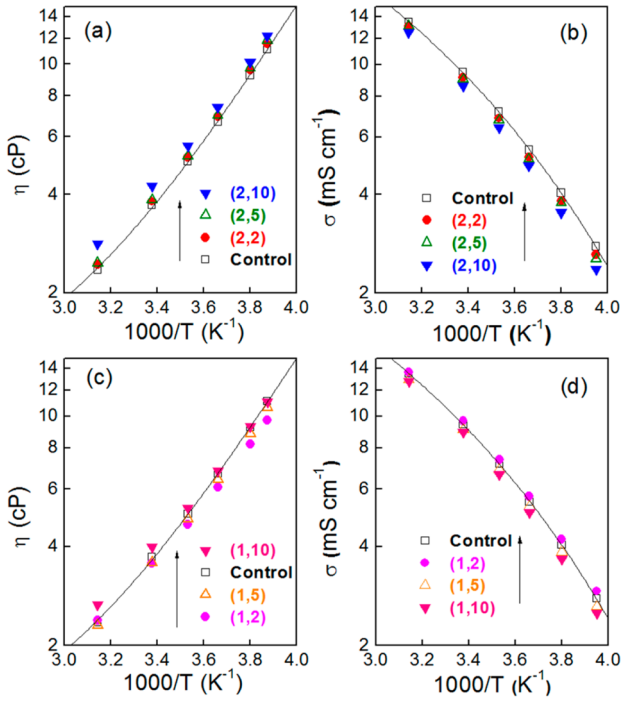

Figure 1. (a, c) Viscosities (η) and (b, d) ionic conductivities (σ) of electrolytes containing aliphatic (a, b) di-nitriles and (c, d) mono-nitriles. (*x*, *y*) indicates the base electrolyte in the presence of nitriles with *x* = the number of nitrile groups and *y* = the number of aliphatic carbons.

and σ are directly related to electrochemical performances of LIBs, it should be checked whether introduction of nitriles into electrolytes change the properties of the base electrolyte. From the viewpoint of temperature dependency, η decreased with increasing temperature while σ increased, following Arrhenius behavior roughly. Serious impairment of the fluidic and transport properties by introducing nitriles into the base electrolyte are not expected when considering high dielectric constant of nitriles[20] (intermediate value between EC and EMC) and their low melting points.[16] There were no significant changes of η and σ observed with nitriles with up to five aliphatic carbons independent of the number of cyano groups. With *m* = 10 or *n* = 10, however, σ decreased slightly with higher values of η for both mono-nitriles and di-nitriles. Therefore, the use of too long chain of aliphatic moiety is not encouraged. With a closer look for comparison, the electrolyte containing mono-nitrile with *m* = 2 or (1, 2) showed a slightly enhanced values of η and σ (3.6 cP; 9.7 mS cm^{-1} at 23 °C), compared with those of the base electrolyte (3.7 cP; 9.5 mS cm^{-1}).

Thermal Stability. Surface of charged or delithiated Li_xCoO_2 (*x* = 0.5) is highly reactive with solvent molecules in electrolytes at excessive high temperature. Electrolyte is electrochemically decomposed with large amount of gas emitted, subsequently leading to capacity fading. More serious progress of the exothermal side-reactions engenders dimensional distortion, cracks in Al pack housing sheets, leakage of

electrolyte and even thermal runaway.[14,21,22] As an effective method to prevent the exothermic side reactions, the use of succinonitrile (SN) as an additive was reported.[14] Thermal stability of LCO|graphite cells containing the base electrolyte in the presence of nitriles were estimated by tracing thickness of the pouch cells stored at 80 °C during 3 days (Figure 2). All of

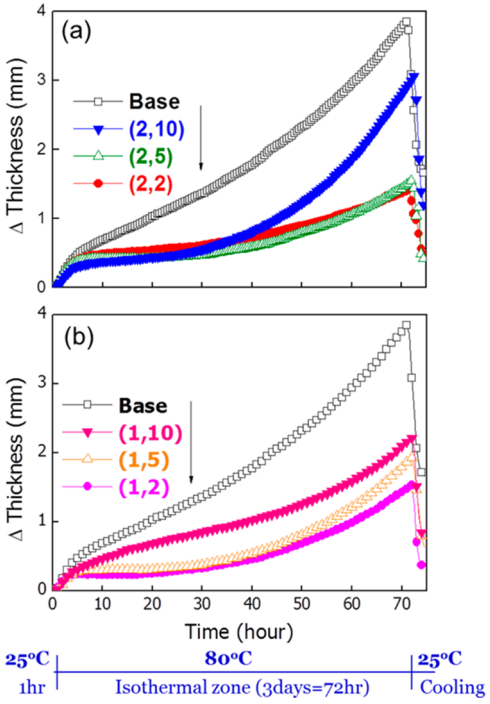

Figure 2. Dimensional change of pouch-type LCO/graphite cells at 80 °C for 3 days with electrolytes containing (a) aliphatic di-nitriles (2, *n*) and (b) aliphatic mono-nitriles (1, *m*). An optimized amount of electrolyte (2.5 cm^3) was injected to all cells, which was determined quantitatively by measuring the uptake amount of electrolyte by electrodes used in assembled LCO|graphite full cells.

the nitrile-present electrolytes showed smaller dimensional expansion than the base electrolyte. The cell thickness change was most serious with the additives at *m* = 10 or *n* = 10 among the nitrile-containing electrolytes. The shorter aliphatic chains (m or *n* = 2 or 5) were favored in terms of the dimensional change for both mono-nitriles and di-nitriles. The smaller dimensional changes at high temperature indicate suppression of gas evolution. The interface modified by nitriles worked effectively in terms of protective layer formation on the surface of LCO. In comparison between nitriles, the di-nitriles were more effective than the mono-nitriles for thermal stability (except of m or *n* = 10): e.g., percentage of maximum expansion with respect to that of base electrolyte = 50 % for (1, 5) versus 40 % for (2, 5).

In addition to side reactions on cathodes, the gas evolution induced by thermal degradation of passivation layer on graphite anodes should be considered. Nitrile molecules did not significantly take part in the formation of solid-electrolyte interphase (SEI) layer. Differential capacity plots (d*Q*/d*V* vs *V* in Figure S1a, b in the Supporting Information) of the SEI layer formation showed there are no distinguished changes of peaks (neither peak shift nor new peaks) between before and after the addition of nitriles. The main formation peaks were caused by cathodic decomposition of FEC. Only thing recognizable was reduction of peak area or charges relevant to the SEI formation. Also, X-ray photoemission spectra (XPS) of N 1s supports no involvement of nitriles in formation of SEI layer on graphite. The nitrogen-related peak was not detected with graphites, whereas it was found with all cathode electrodes from nitrile-present cells (Figures S2 and S3 in the Supporting Inforation). Therefore, the dimensional changes in thickness of the soft-packed cells at high temperature are mainly attributed to the interfacial reactivity of electrolyte contacted with cathode. Different from the aliphatic nitriles, however, alkene-containing nitriles (e.g. *cis*, *cis*-muconontrile) were decomposed prior to FEC during the SEI layer formation process, delivering inferior capacities (see Figure S4a, b in the Supporting Information).

Surface Coverage of Nitrile Molecules on Cathode Surface. The dependency of thermal stability on aliphatic chain length (*m* or *n*) can be understood from the viewpoint of coverage of nitrile molecules adsorbed on the LCO surface (Figure 3). In the absence of nitriles (Figure 3a), solvent

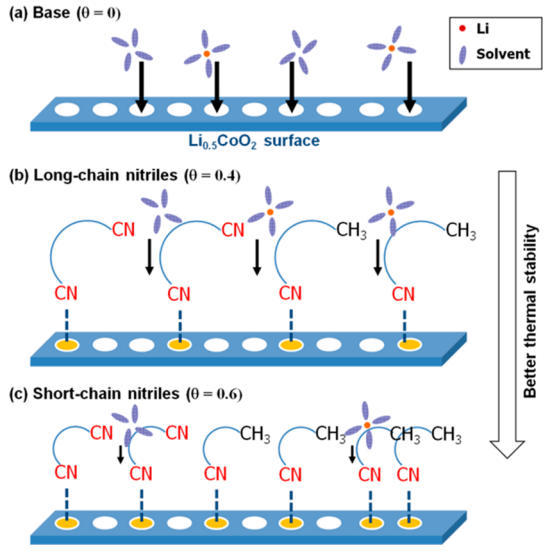

Figure 3. Effects of coverage (θ) by nitrile adsorption and steric hindrance of aliphatic chains of nitriles on protecting cathode surface from electrolyte. Electrolyte accessibility into cathode surface was described in (a) nitrile-absent electrolyte and nitrile-present electrolytes of (b) long-chain nitriles and (c) short-chain nitriles.

molecules (carbonates) or Li^+-associated solvent molecules contact delithiated $Li_{0.5}CoO_2$ surface directly, leading to side reactions emitting gases at a thermal condition. In the presence of nitrile molecules, however, the direct contact of the solvent molecules is suppressed. Prior to the solvent molecules, the nitrile molecules are adsorbed on the delithiated, so partially positively charged, surface of cathode. The strongly preferred adsorption is driven by the electronegativity of nitrile groups (−CN).[14] The degree of preventing solvent molecules from direct access to the surface (that is to say, thermal stability) probably depends on the surface coverage (θ) of nitrile molecules and steric hindrance of their aliphatic chains. The higher θ or larger molecular volume blocks the direct access of solvent molecules more significantly. As the chain length proportional to the number of carbons (*m* or *n*) increases, θ decreases with steric hindrance increasing. Therefore, effects of the two factors on thermal stability are traded off in a certain range of m or n values. With *m* or *n* = 10, the value of θ is too small to cover the cathode surface efficiently (Figure 3b). The steric hindrance of long nitrile molecules blocks not only direct

contact of solvent molecules but also, even more seriously, additional adsorption of nitrile molecules. Less coverage by nitrile molecules exposes intact surface to electrolyte, leading to side reactions. With m or n = 2 and 5, higher coverages were reached and aliphatic chains of the compact adsorption layer hinder the access of solvent molecules also suppress the contact between electrolyte and electrode surface (Figure 3c). The similar level of thermal stability between m or n = 2 and 5 was obtained because the blocking effects results from summation of the two factors, θ and steric hindrance, which have counter-directional m or n dependency.

To confirm the coverage effect on thermal stability, we investigated the concentration dependency (Figure 4). The

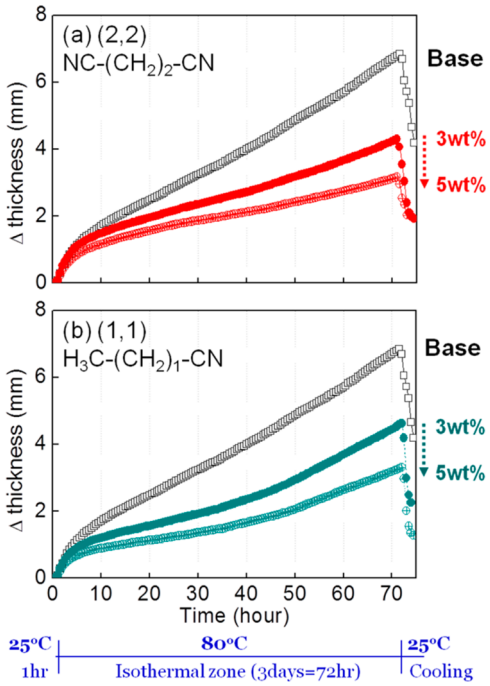

Figure 4. Dimensional change of pouch-type LCO/graphite cells at 80 °C for 3 days with electrolytes containing succinonitrile (2, 2) (a) and propionitrile (1, 1) (b) with two different concentrations (3 and 5 wt %). Base electrolyte was included for comparison. An excessive amount of electrolyte (totally 3.5 cm^3 with 1.0 cm^3 excess) was used to identify the change of cell thickness clearly.

adsorption amount or θ is determined by equilibrium between species in solution phase and adsorbed species so that higher concentration of nitriles in electrolyte leads to higher θ. Succinonitrile (n =2) and propionitrile (m =1) were used as representative molecules of di-nitriles and mono-nitriles, respectively. Excessive amounts of electrolytes more than those used in other experiments (e.g., Figure 2) were injected to soft-packed cells of LCO/graphite to investigate difference of gas swelling distinctively. Dimensional changes caused by gas evolution decreased with increasing concentration of both di-nitriles and mono-nitriles. While the change of cell thickness (Δthickness) with the base electrolyte reached 6.85 mm at its maximum, both succinonitrile and propionitrile-present electrolytes ((2, 2) and (1, 1)) suppressed the swelling behavior with inversed concentration-dependency: Δthickness = 4.3 mm for 3 wt % and 3.2 mm for 5 wt % with succinonitrile; 4.6 mm for 3 wt % and 3.3 mm for 5 wt % with propionitrile. Therefore, the surface coverage of adsorbed nitrile molecules is proven as the dominant factor to determine thermal stability. It should be notified that the 5 wt % of (2, 2) and (1, 1) is not optimized value. Trade-off between enhanced thermal stability and inferior performances caused by lower ionic conductivities should be considered when the use of more amount of nitriles is tried.

Safety at High Temperature. Thermal reactivity of charged $Li_{0.5}CoO_2$ cathodes soaked in electrolytes was investigated by DSC (Figure 5). Exothermic reactions were

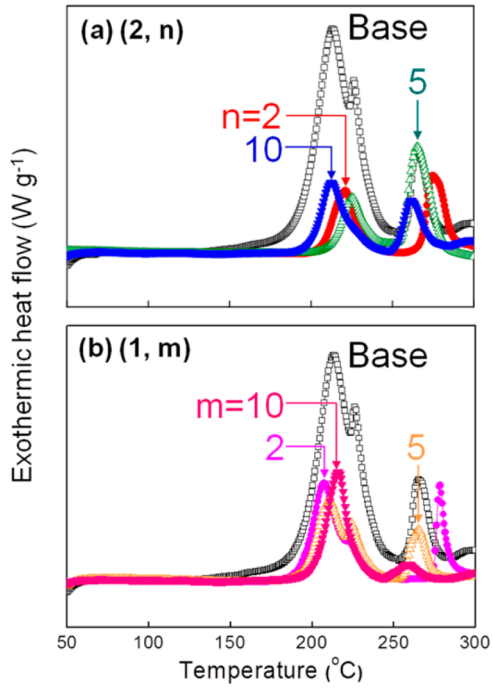

Figure 5. Heat flow profiles of exothermic reactions between fully charged Li_xCoO_2 (x = 0.5) and electrolyte in the absence and presence of nitrile molecules. (a) Di-nitrile-containing electrolytes (2, n). (b) Mono-nitrile-containing electrolytes (1, m). The base electrolytes were included for comparison (black squares).

initiated at 130 °C with the base electrolyte. Subsequently, oxygen released by cathode decomposition reacts violently with the electrolyte, accompanying with a considerable amount of enthalpy change (ΔH) with two exothermic peaks at 213 and 265 °C.[22−27] With the nitrile-present electrolytes, the onset temperatures of exothermic reactions were shifted to higher temperatures and exothermic heat was less released. The retarded initiation of exothermic reactions should be emphasized because the initial heat breaks thermal balance of LIBs. Delay of the onset temperature saves time to dissipate influxed heat at a temporary thermal shock, preventing heat accumulation within cells and maintaining thermally stable state. With energy generation term caused by interfacial side reactions beyond a dissipation limit, however, the rate of heat accumulation is self-accelerated. Cells are then introduced into the track of thermal runaway.

The onset temperatures were significantly shifted with nitrile additives from that of the base electrolyte. The onset temperature of the base electrolyte at 130 °C moved to around 200 °C for n = 2 and 5 and 190 °C for n = 10 in di-nitriles (Figure 5a). In addition, the di-nitrile-present electrolytes (2, n) generated only 18 % of energy that the base electrolyte did: peak area ≈ 220 J g^{-1} on average for (2, n)

versus 1200 J g^{-1} for the base electrolyte. Qualitatively similar thermal behaviors were obtained with the mono-nitrile-containing electrolytes (Figure 5b). The onset temperatures were estimated around 180 °C for m = 2 and 5 and 186 °C for m = 10. About 34 % of heat (~400 J g^{-1}) was generated compared with the base electrolyte. Di-nitriles secured thermal safety better than mono-nitriles in the same length of aliphatic chain, which would be related to thermal stability of adsorbed layer consisting of the nitriles. The superiority of di-nitriles to mono-nitriles is consistent between thermal stability beyond 150 °C (Figure 5) and during 3-day storage at 80 °C (Figure 2). Concentration of −C≡N in di-nitriles is twofold as high as that of mono-nitriles at an identical molar fraction. There is every possibility that more amount of di-nitrile molecules were adsorbed to form denser surface layer.[14]

High-Temperature Performance. With advantages of low gas generation and small exothermic heat evolution in the nitrile-assistant electrolytes, discharge capacities at 1C were traced at 60 °C along cycles (Figure 6). All of the nitrile-assistant electrolytes, except of the mono-nitrile with long aliphatic chain (1, 10), was superior to the base electrolyte in terms of cyclic retention of capacity. The base electrolyte experienced severe capacity decay even at the initial cycles at such a high temperature, showing 60 and 14% retention at the 1st and the 300th cycle. There were no distinctive differences between mono-nitriles and di-nitriles for m or n = 2 and 5: ~85 % retention at the 300th cycle. The deteriorated capacity retention of the base electrolyte is mainly attributed to vigorous reactions of carbonate solvent molecules with delithiated cathode. At elevated temperatures, the electrolyte molecules are highly oxidized and decomposed, resulting in gas emission, electrolyte depletion and lithium metal dendrite growth. On the contrary, the cathode surface covered by Co-CN complex rarely permits carbonates to react with the $Li_{0.5}CoO_2$.

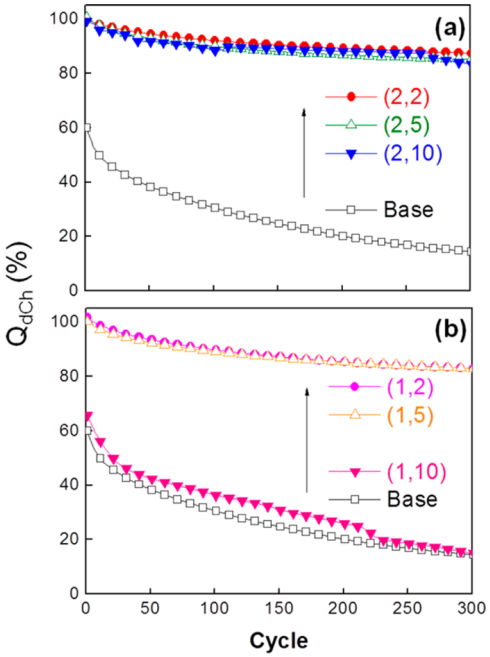

Figure 6. Cyclic performances of pouch-type LCO|graphite cells at 60 °C. (a) Di-nitrile-containing electrolytes (2, n). (b) Mono-nitrile-containing electrolytes (1, m). The base electrolyte was included for comparison. The cells were charged and discharged at 1C between 3 and 4.2 V. Potential profiles during charge and discharge at each cycle were provided in Figure S5 in the Supporting Information.

Different from other nitrile-containing electrolytes (especially its di-nitrile counterpart (2, 10)), the mono-nitrile of the longest aliphatic chain (1, 10) showed serious decay of capacity like the base electrolyte (Figure 6b). The capacity decay is not exactly understood by coverage and steric hindrance because (1,10) was better than or at least similar to (2, 10) in terms of gas evolution caused by side-reactions (Figure 2). Nonpolar properties of long aliphatic chain would be helpful to explain the contradictory results between suppressed gas evolution and poor cyclability. The nonpolarity of dodecanenitrile used in (1, 10) possibly hinder the access of polar electrolyte such as carbonates. Even if dodecanenitrile is soluble in carbonate solvents due to its cyano group, its polarity becomes extremely weaker after being immobilized on LCO surface by the interaction between −CN and Co. On the other hand, dodecanedinitrile used in (2, 10) does not develop ionic resistance after adsorption because at least a portion of the (2, 10) still has the other nitrile groups exposed to electrolyte. For the same reason, the capacity of cells based on (1, 10) at room temperature was also inferior to that of the base electrolyte: ~760 mAh g^{-1} for (1, 10) versus ~770 mAh g^{-1} for the base electrolyte.

Impedance spectra measured after storage at 80 °C for 3 days (Figure 7) supported the results of cyclic performances (Figure 6; see Figure S7 in the Supporting Information for the spectra before the thermal storage). All nitrile-present electrolytes

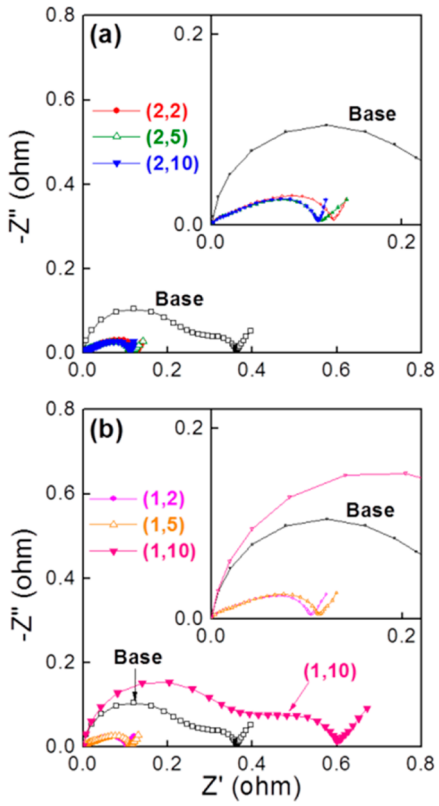

Figure 7. Impedance spectra of fully charged cells after long-term storage at 80 °C. (a) Di-nitrile-containing electrolytes (2, n). (b) Mono-nitrile-containing electrolytes (1, m). The base electrolyte as a control was indicated in (a) and (b). A possible equivalent circuit to describe the spectra is given in Figure S6.

except of the dodecanenitrile showed impedances significantly smaller than the base electrolyte. Formation of resistive passive layer resulting from thermal decomposition of electrolyte on charged surface of electrodes would explain the large impedance of the base electrolyte. However, the impedances relevant to charge transfer resistances (R_{CT}) on cathodes and anodes in dodecanenitrile-containing electrolyte (1, 10) was larger than those of the base electrolyte. The result is consistent with the serious capacity decay with cycles in (1, 10) (Figure 6b). Recovery of capacities of cells thermally stored at 80 °C for 3 days was also enhanced with nitrile molecules (Figure 8).

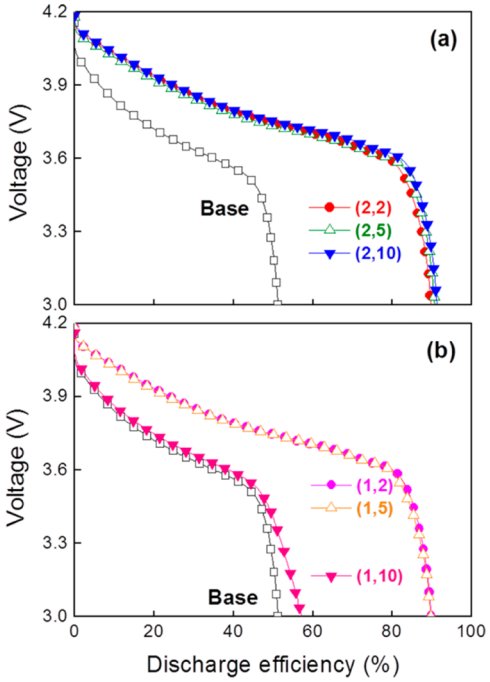

Figure 8. Capacity recovery after the thermal storage at 80 °C for 3 days. (a) Di-nitrile-containing electrolytes (2, *n*). (b) Mono-nitrile-containing electrolytes (1, *m*). The base electrolyte was included for comparison. Capacity was normalized by the capacity measured before the thermal storage. All cells were charged at 0.2*C* and then discharged at 0.2*C*. Potential profiles during charges are shown in Figure S8 in the Supporting Information.

After the thermal storage, discharge capacity of the base electrolyte decreased to ~50% of capacity measured before the thermal storage. Because of thermally induced formation of passive layer on cathode, LCO|graphite cell in the conventional base electrolyte suffered from large IR drop and severe capacity fading. However, cells containing nitrile-assistant electrolytes (except of dodecanenitrile) showed ~90 % recovery. The nonpolar long-chain nitrile (dodecanenitrile) delivered ~57 % recovery.

Surface Coverage (θ) Estimated by Higher Oxidation States of Cobalt Atoms. The XPS spectra of N 1s (see Figure S2 in the Supporting Information) and Co 2p (Figure 9) of delithiated $LiCoO_2$ surfaces were measured with or without nitriles. All samples were rinsed thoroughly with EMC under a moisture-free environment (H_2O < 1ppm) to eliminate a surplus of nitrile molecules which never form a strong bond between −CN and Co.[14] The N 1s signals were definitely observed at about 399 eV in the all samples from nitrile-containing cells, while the peaks of the nitrile-absent counterparts were not clearly detected (see Figure S2 in the Supporting

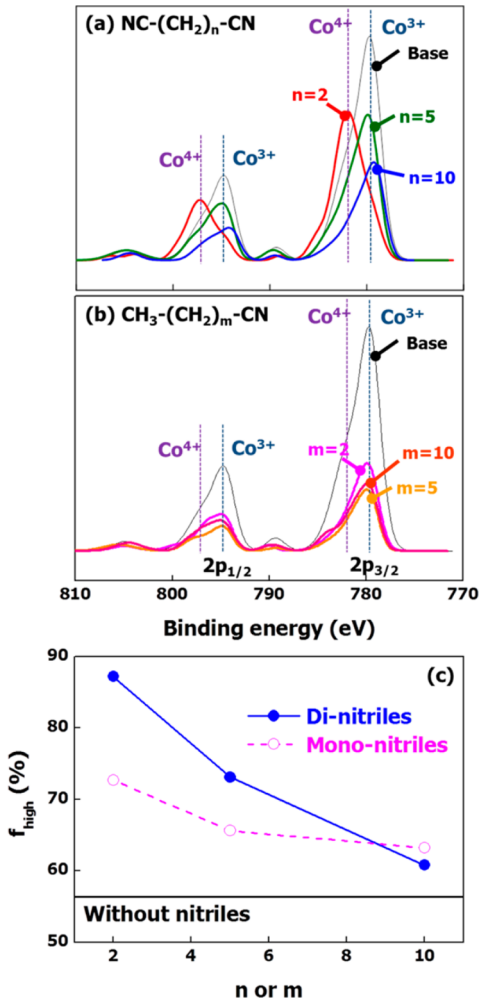

Figure 9. (a, b) X-ray photoemission spectra of Co 2p of delithiated Li_xCoO_2 surface (x = 0.5) in the electrolyte solution with aliphatic (a) di-nitriles and (b) mono-nitriles, respectively. The spectra of base electrolyte without nitriles were indicated. (c) Fraction (f_{high}) of higher oxidation states (Co^{4+} and $Co^{(4+\delta)+}$) of cobalt atoms as a function of the carbon number of aliphatic chains of nitriles (n or m).

Information). The spilt Co 2p peaks, consisting of Co $2p_{3/2}$ and Co $2p_{1/2}$ due to spin-orbit coupling, were clearly observed in all samples. They are also subdivided into two oxidized Co states, Co^{4+} and Co^{3+}, through peak deconvolution optimization (see Figure S9 and Table S1 in the Supporting Information).[28] With the nitrile-absent electrolyte (base), two Co 2p peaks were clearly observed at 779.5 eV (Co $2p_{3/2}$) and at 794.5 eV (Co $2p_{1/2}$). The relative peak area fractions were 43.6 % for Co^{3+} and 56.4 % for Co^{4+} on average, confirming Li_xCoO_2 at x = ~0.5. With the nitrile-present electrolytes, on the contrary, additional species $Co^{4+\delta}$ were required for satisfactory goodness of fit related to peak deconvolution. More positively charged species including $Co^{4+\delta}$ as well as Co^{4+} were predominant over Co^{3+}. With succinonitrile (n=2) as a representative example, the peak shift to higher binding energy responsible for more positively charged species was clear with Co $2p_{3/2}$ at 782 eV and Co $2p_{1/2}$ at 797 eV. Peak area fractions were estimated at 4.9 % for $Co^{4+\delta}$ and 82.3 % for Co^{4+} versus 12.8% for Co^{3+} on average. Therefore, it can be concluded that more positively charged species were developed in the presence of nitrile molecules.

More dominant portion of Co^{4+} and $Co^{(4+\delta)+}$ over Co^{3+} confirms the effective charge balancing mechanism induced by the electronegativity of nitrile functionality during delithiation processes.[14] The electronegative cloud of the nitrile functionality is coupled with a cobalt atom on surface to form CN-Co complex. Higher electron density of the complex is developed by charge donation of -δ from the nitrile to the cobalt atom. During delithiation or oxidation processes, the extra charge of the complex is extracted to form the more oxidized state $Co^{(4+\delta)+}$ on surface in order to balance charges between the surface and bulk cobalt atoms. Therefore, the surface coverage θ of nitriles can be estimated by the portion (f_{high}) of higher oxidized states (Co^{4+} and $Co^{(4+\delta)+}$) of cobalt atoms. The decrease in f_{high} with n or m (Figure 9c) is reasonably accepted because smaller molecules occupy higher coverage with experiencing less steric hindrance between the molecules. Also, it should be considered that the smaller molar concentrations were used with longer aliphatic chains (the weight percentage was fixed.).

CONCLUSION

We demonstrated that nitrile-assistant electrolytes improved the thermal stability of LCO|graphite cells without sacrificing performances. Electrolytes containing either aliphatic mononitriles or di-nitriles have excellent tolerance against thermal abuse by protecting the surface of LCO from thermally-induced side reactions. The effects of the aliphatic chain length of the nitriles were determined by balancing between surface coverage θ and steric hindrance. As a result, nitriles containing two and five aliphatic carbons, independent of the number of nitrile groups, showed similar thermal stability and performances. In cases of nitriles of long aliphatic chains such as ten aliphatic carbons, however, the polarity of the ending group of nitrile molecules should have been considered in addition to the previous two factors. Dodecanenitrile-present electrolyte was significantly inferior to other nitriles even if the gas generation was suppressed. The behavior was much different from that of its di-nitrile counterpart (dodecanedinitrile-containing electrolyte). The alkane ending groups of dodecanenitrile are considered to discourage the access of lithium ions into the cathode material while the nitrile ending groups of adsorbed dodecanedinitrile provide environments favorable to the lithium ion penetration. Therefore, the structure of surface coverage molecules to protect cathode materials can be optimally designed by considering those three factors. Nitriles containing branched aliphatic chains with nitrile ending groups or cyanoresins would be candidates as the thermal stability enhancer. We believe that incorporation of aliphatic mononitriles or di-nitriles as an additive in electrolyte is a simple yet very attractive strategy actualizing safer LIBs without any capacity loss.

ASSOCIATED CONTENT

Supporting Information

Information of Co 2p peaks, differential capacity curves, N 1s spectra of $Li_{0.5}CoO_2$ and graphite by XPS, electrochemical data of cells in the presence of non-aliphatic nitriles, potential profiles during charge and discharge, a proposed equivalent circuit, impedance spectra at 23 °C before thermal storage, peak deconvolution of Co2P XPS spectra, rate capabilities at room temperature. This material is available free of charge via the Internet at http://pubs.acs.org/.

AUTHOR INFORMATION

Corresponding Author

*E-mail: philiphobi@hotmail.com.

Notes

The authors declare no competing financial interest.

ACKNOWLEDGMENTS

This work was supported by MOTIE (Star:20135020900030) and MOE (BK21Plus:META, 10Z20130011057), Korea.

REFERENCES

(1) Sun, Y. K.; Myung, S. T.; Park, B. C.; Prakash, J.; Belharouak, I.; Amine, K. High-Energy Cathode Material for Long-Life and Safe Lithium Batteries. *Nat. Mater.* **2009**, *8*, 320−324.

(2) Takahashi, Y.; Tode, S.; Kinoshita, A.; Fujimoto, H.; Nakane, I.; Fujitani, S. Development of Lithium-Ion Batteries with a $LiCoO_2$ Cathode toward High Capacity by Elevating Charging Potential. *J. Electrochem. Soc.* **2008**, *155*, A537−A541.

(3) Kannan, A. M.; Rabenberg, L.; Manthiram, A. High Capacity Surface-Modified $LiCoO_2$ Cathodes for Lithium-Ion Batteries. *Electrochem. Solid-State Lett.* **2003**, *6*, A16−A18.

(4) Barpanda, P.; Nishimura, S.; Yamada, A. High-Voltage Pyrophosphate Cathodes. *Adv. Energy Mater.* **2012**, *2*, 841−859.

(5) Hao, X. G.; Bartlett, B. M. Improving the Electrochemical Stability of the High-Voltage Li-Ion Battery Cathode $LiNi_{0.5}Mn_{1.5}O_4$ by Titanate-Based Surface Modification. *J. Electrochem. Soc.* **2013**, *160*, A3162−A3170.

(6) Manthiram, A.; Chemelewski, K.; Lee, E.-S. A Perspective on the High-Voltage $LiMn_{1.5}Ni_{0.5}O_4$ Spinel Cathode for Lithium-Ion Batteries. *Energy Environ. Sci.* **2014**, *7*, 1339−1350.

(7) Lee, J. I.; Lee, E. H.; Park, J. H.; Park, S.; Lee, S. Y. Ultrahigh-Energy-Density Lithium-Ion Batteries Based on a High-Capacity Anode and a High-Voltage Cathode with an Electroconductive Nanoparticle Shell. *Adv. Energy Mater.* **2014**, DOI: 10.1002/aenm.201301542.

(8) Zhang, Z.; Fouchard, D.; Rea, J. Differential Scanning Calorimetry Material Studies: Implications for the Safety of Lithium-Ion Cells. *J. Power Sources* **1998**, *70*, 16−20.

(9) Aurbach, D.; Markovsky, B.; Salitra, G.; Markevich, E.; Talyossef, Y.; Koltypin, M.; Nazar, L.; Ellis, B.; Kovacheva, D. Review on Electrode-Electrolyte Solution Interactions, Related to Cathode Materials for Li-Ion Batteries. *J. Power Sources* **2007**, *165*, 491−499.

(10) Zhang, S. S. A Review on Electrolyte Additives for Lithium-Ion Batteries. *J. Power Sources* **2006**, *162*, 1379−1394.

(11) Wong, D. H.; Thelen, J. L.; Fu, Y.; Devaux, D.; Pandya, A. A.; Battaglia, V. S.; Balsara, N. P.; DeSimone, J. M. Nonflammable Perfluoropolyether-Based Electrolytes for Lithium Batteries. *Proc. Natl. Acad. Sci. U. S. A.* **2014**, 201314615.

(12) Hyung, Y. E.; Vissers, D. R.; Amine, K. Flame-Retardant Additives for Lithium-Ion Batteries. *J. Power Sources* **2003**, *119*, 383−387.

(13) Zhang, H.; Xia, Q.; Wang, B.; Yang, L.; Wu, Y.; Sun, D.; Gan, C.; Luo, H.; Bebeda, A.; Ree, T. v. Vinyl-Tris-(Methoxydiethoxy) Silane as an Effective and Ecofriendly Flame Retardant for Electrolytes in Lithium Ion Batteries. *Electrochem. Commun.* **2009**, *11*, 526−529.

(14) Kim, Y. S.; Kim, T. H.; Lee, H.; Song, H. K. Electronegativity-Induced Enhancement of Thermal Stability by Succinonitrile as an Additive for Li Ion Batteries. *Energy Environ. Sci.* **2011**, *4*, 4038−4045.

(15) Kim, Y. S.; Cho, Y. G.; Odkhuu, D.; Park, N.; Song, H. K. A Physical Organogel Electrolyte: Characterized by in Situ Thermo-Irreversible Gelation and Single-Ion-Predominent Conduction. *Sci. Rep.* **2013**, *3*, 1917.

(16) Duncan, H.; Salem, N.; Abu-Lebdeh, Y. Electrolyte Formulations Based on Dinitrile Solvents for High Voltage Li-Ion Batteries. *J. Electrochem. Soc.* **2013**, *160*, A838−A848.

(17) Abu-Lebdeh, Y.; Davidson, I. High-Voltage Electrolytes Based on Adiponitrile for Li-Ion Batteries. *J. Electrochem. Soc.* **2009**, *156*, A60−A65.
(18) Abu-Lebdeh, Y.; Davidson, I. New Electrolytes Based on Glutaronitrile for High Energy/Power Li-Ion Batteries. *J. Power Sources* **2009**, *189*, 576−579.
(19) Wang, Q.; Zakeeruddin, S. M.; Exnar, I.; Gratzel, M. 3-Methoxypropionitrile-Based Novel Electrolytes for High-Power Li-Ion Batteries with Nanocrystalline $Li_4Ti_5O_{12}$ Anode. *J. Electrochem. Soc.* **2004**, *151*, A1598−A1603.
(20) Harju, T. O.; KorppiTommola, J. E. I.; Huizer, A. H.; Varma, C. Barrier Crossing Reaction of Electronically Excited $DBMBF_2$ in n-Nitriles: The Role of Solvent Polarity on Activation Energy. *J. Phys. Chem.* **1996**, *100*, 3592−3600.
(21) Armand, M.; Endres, F.; MacFarlane, D. R.; Ohno, H.; Scrosati, B. Ionic-Liquid Materials for the Electrochemical Challenges of the Future. *Nat. Mater.* **2009**, *8*, 621−629.
(22) Balakrishnan, P.; Ramesh, R.; Prem Kumar, T. Safety Mechanisms in Lithium-Ion Batteries. *J. Power Sources* **2006**, *155*, 401−414.
(23) Baba, Y.; Okada, S.; Yamaki, J.-i. Thermal Stability of Li_XCoO_2 Cathode for Lithium Ion Battery. *Solid State Ionics* **2002**, *148*, 311−316.
(24) Shigematsu, Y.; Kinoshita, S.-i.; Ue, M. Thermal Behavior of a C/ $LiCoO_2$ Cell, Its Components, and Their Combinations and the Effects of Electrolyte Additives. *J. Electrochem. Soc.* **2006**, *153*, A2166−A2170.
(25) Yamaki, J.-i.; Baba, Y.; Katayama, N.; Takatsuji, H.; Egashira, M.; Okada, S. Thermal Stability of Electrolytes with Li_XCoO_2 Cathode or Lithiated Carbon Anode. *J. Power Sources* **2003**, *119*, 789−793.
(26) Botte, G. G.; White, R. E.; Zhang, Z. Thermal Stability of $LiPF_6$−EC: EMC Electrolyte for Lithium Ion Batteries. *J. Power Sources* **2001**, *97*, 570−575.
(27) Wang, Q.; Sun, J.; Chen, X.; Chu, G.; Chen, C. Effects of Solvents and Salt on the Thermal Stability of Charged $LiCoO_2$. *Mater. Res. Bull.* **2009**, *44*, 543−548.
(28) Dupin, J.; Gonbeau, D.; Benqlilou-Moudden, H.; Vinatier, P.; Levasseur, A. XPS Analysis of New Lithium Cobalt Oxide Thin-Films before and after Lithium Deintercalation. *Thin Solid Films* **2001**, *384*, 23−32.